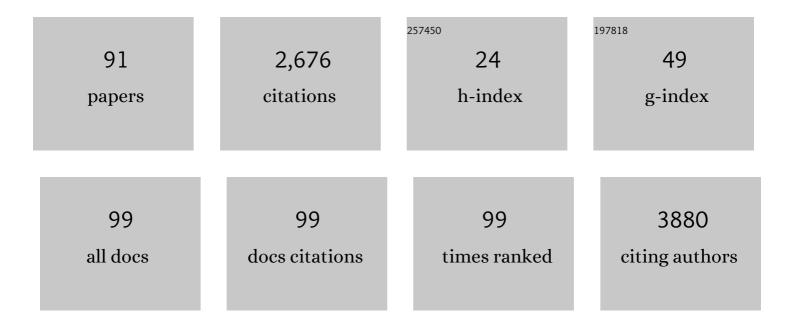
## Zhi-Cheng Li

List of Publications by Year in descending order

Source: https://exaly.com/author-pdf/9163553/publications.pdf Version: 2024-02-01



7HI-CHENCLI

#	Article	IF	CITATIONS
1	Predicting 1p/19q co-deletion status from magnetic resonance imaging using deep learning in adult-type diffuse lower-grade gliomas: a discovery and validation study. Laboratory Investigation, 2022, 102, 154-159.	3.7	8
2	Glioma survival prediction from whole-brain MRI without tumor segmentation using deep attention network: a multicenter study. European Radiology, 2022, 32, 5719-5729.	4.5	10
3	Generative Adversarial Networks in Medical Image augmentation: A review. Computers in Biology and Medicine, 2022, 144, 105382.	7.0	118
4	A computational toolset for rapid identification of SARS-CoV-2, other viruses and microorganisms from sequencing data. Briefings in Bioinformatics, 2021, 22, 924-935.	6.5	34
5	Enhancing the X-Ray Differential Phase Contrast Image Quality With Deep Learning Technique. IEEE Transactions on Biomedical Engineering, 2021, 68, 1751-1758.	4.2	10
6	Validation of CT radiomics for prediction of distant metastasis after surgical resection in patients with clear cell renal cell carcinoma: exploring the underlying signaling pathways. European Radiology, 2021, 31, 5032-5040.	4.5	14
7	GaLNet: Weakly-Supervised Learning for Evidence-Based Tumor Grading and Localization in MR Imaging. Communications in Computer and Information Science, 2021, , 249-258.	0.5	0
8	DeepPhase: Learning phase contrast signal from dual energy X-ray absorption images. Displays, 2021, 69, 102027.	3.7	7
9	Biologic Pathways Underlying Prognostic Radiomics Phenotypes from Paired MRI and RNA Sequencing in Glioblastoma. Radiology, 2021, 301, 654-663.	7.3	38
10	Dual-region radiomics signature: Integrating primary tumor and lymph node computed tomography features improves survival prediction in esophageal squamous cell cancer. Computer Methods and Programs in Biomedicine, 2021, 208, 106287.	4.7	18
11	Deep learning features from diffusion tensor imaging improve glioma stratification and identify risk groups with distinct molecular pathway activities. EBioMedicine, 2021, 72, 103583.	6.1	31
12	Deep Learning Radiomics to Predict PTEN Mutation Status From Magnetic Resonance Imaging in Patients With Glioma. Frontiers in Oncology, 2021, 11, 734433.	2.8	10
13	Synthesis of a Micro-Crosslinked Polyacrylamide Flocculant and Its Application in Treatment of Oily Produced Water. Energy & Fuels, 2021, 35, 18396-18405.	5.1	6
14	Identification of a Qualitative Signature for the Diagnosis of Dementia With Lewy Bodies. Frontiers in Genetics, 2021, 12, 758103.	2.3	1
15	Radiomics and Qualitative Features From Multiparametric MRI Predict Molecular Subtypes in Patients With Lower-Grade Glioma. Frontiers in Oncology, 2021, 11, 756828.	2.8	12
16	Combining DWI radiomics features with transurethral resection promotes the differentiation between muscle-invasive bladder cancer and non-muscle-invasive bladder cancer. European Radiology, 2020, 30, 1804-1812.	4.5	41
17	Radiomic Features From Multi-Parameter MRI Combined With Clinical Parameters Predict Molecular Subgroups in Patients With Medulloblastoma. Frontiers in Oncology, 2020, 10, 558162.	2.8	34
18	Radiomics nomogram for preoperative prediction of progression-free survival using diffusion-weighted imaging in patients with muscle-invasive bladder cancer. European Journal of Radiology, 2020, 131, 109219.	2.6	17

ZHI-CHENG LI

#	Article	IF	CITATIONS
19	Incremental prognostic value and underlying biological pathways of radiomics patterns in medulloblastoma. EBioMedicine, 2020, 61, 103093.	6.1	23
20	Evaluation of reconstruction algorithms for a stationary digital breast tomosynthesis system using a carbon nanotube X-ray source array. Journal of X-Ray Science and Technology, 2020, 28, 1157-1169.	1.0	3
21	Deep Learning vs. Radiomics for Predicting Axillary Lymph Node Metastasis of Breast Cancer Using Ultrasound Images: Don't Forget the Peritumoral Region. Frontiers in Oncology, 2020, 10, 53.	2.8	146
22	3D Deep Residual Encoder-Decoder CNNS with Squeeze-and-Excitation for Brain Tumor Segmentation. Lecture Notes in Computer Science, 2020, , 234-243.	1.3	1
23	Automatic image-domain Moiré artifact reduction method in grating-based x-ray interferometry imaging. Physics in Medicine and Biology, 2019, 64, 195013.	3.0	16
24	<p>Genetic Biomarkers For Hepatocellular Carcinoma In The Era Of Precision Medicine</p> . Journal of Hepatocellular Carcinoma, 2019, Volume 6, 151-166.	3.7	25
25	A Comparative Study of CNN-Based Super-Resolution Methods in MRI Reconstruction. , 2019, , .		2
26	Towards an Interpretable Radiomics Model for Classifying Renal Cell Carcinomas Subtypes: A Radiogenomics Assessment. , 2019, , .		1
27	3D Deep Attention Network for Survival Prediction from Magnetic Resonance Images in Glioblastoma. , 2019, , .		7
28	Gencore: an efficient tool to generate consensus reads for error suppressing and duplicate removing of NGS data. BMC Bioinformatics, 2019, 20, 606.	2.6	43
29	Differentiation of clear cell and non-clear cell renal cell carcinomas by all-relevant radiomics features from multiphase CT: a VHL mutation perspective. European Radiology, 2019, 29, 3996-4007.	4.5	78
30	Multiregional radiomics features from multiparametric MRI for prediction of MGMT methylation status in glioblastoma multiforme: A multicentre study. European Radiology, 2018, 28, 3640-3650.	4.5	131
31	NIMG-14. MULTIREGIONAL RADIOMICS PROFILING FROM MULTIPARAMETRIC MRI: IDENTIFYING AN IMAGING PREDICTOR OF IDH1 MUTATION STATUS IN GLIOBLASTOMA MULTIFORME. Neuro-Oncology, 2018, 20, vi178-vi178.	1.2	0
32	Multiregional radiomics profiling from multiparametric MRI: Identifying an imaging predictor of IDH1 mutation status in glioblastoma. Cancer Medicine, 2018, 7, 5999-6009.	2.8	72
33	Effect of Osmotic Pressure on Migration Behavior of nZnO in GCLs. Advances in Civil Engineering, 2018, 2018, 1-9.	0.7	1
34	Comparison of Transferred Deep Neural Networks in Ultrasonic Breast Masses Discrimination. BioMed Research International, 2018, 2018, 1-9.	1.9	107
35	Experiment on sealing efficiency of carbon fiber composite grout under flowing conditions. Construction and Building Materials, 2018, 182, 43-51.	7.2	27
36	A Fully-Automatic Multiparametric Radiomics Model: Towards Reproducible and Prognostic Imaging Signature for Prediction of Overall Survival in Glioblastoma Multiforme. Scientific Reports, 2017, 7, 14331.	3.3	101

Zhi-Cheng Li

#	Article	IF	CITATIONS
37	A Deep Learning-Based Radiomics Model for Prediction of Survival in Glioblastoma Multiforme. Scientific Reports, 2017, 7, 10353.	3.3	432
38	Automatic Extraction of MRI Radiomics Features in Glioblastoma Multiforme: A Reproducibility Evaluation. , 2017, , .		0
39	Identifying a radiomics imaging signature for prediction of overall survival in glioblastoma multiforme. , 2017, , .		1
40	Iterative image-domain ring artifact removal in cone-beam CT. Physics in Medicine and Biology, 2017, 62, 5276-5292.	3.0	42
41	Variants in <i>ANRIL</i> gene correlated with its expression contribute to myocardial infarction risk. Oncotarget, 2017, 8, 12607-12619.	1.8	34
42	A vessel segmentation method for multi-modality angiographic images based on multi-scale filtering and statistical models. BioMedical Engineering OnLine, 2016, 15, 120.	2.7	17
43	Clustering of MRI Radiomics Features for Glioblastoma Multiforme: An Initial Study. Lecture Notes in Computer Science, 2016, , 311-319.	1.3	1
44	Older, vulnerable patient view: a pilot and feasibility study of the patient measure of safety (PMOS) with patients in Australia. BMJ Open, 2016, 6, e011069.	1.9	10
45	Edge-aware Local Laplacian Filters for Medical X-Ray Image Enhancement. Lecture Notes in Computer Science, 2016, , 102-108.	1.3	2
46	Deepening our Understanding of Quality in Australia (DUQuA): a study protocol for a nationwide, multilevel analysis of relationships between hospital quality management systems and patient factors. BMJ Open, 2015, 5, e010349.	1.9	18
47	Facile method for investigating electrochemically induced products in films deposited directly on grids as working electrodes. Materials Letters, 2015, 157, 1-3.	2.6	1
48	Accurate kidney surface reconstruction from 3D ultrasonography for volume assessment: First clinical evaluation. , 2015, 2015, 2981-4.		0
49	Cluster Randomized Controlled Trial of An Aged Care Specific Leadership and Management Program to Improve Work Environment, Staff Turnover, and Care Quality. Journal of the American Medical Directors Association, 2015, 16, 629.e19-629.e28.	2.5	40
50	Resource allocation with beamforming technique for MDC multicast in OFDM-based CRNs. , 2014, , .		3
51	Augmented reality using 3D shape model for ultrasound-guided percutaneous renal access: A pig model study. , 2014, , .		2
52	Phase evolution of magnetron sputtered nanostructured ATO on grid during lithiation–delithiation processes as model electrodes for Li-ion battery. Physical Chemistry Chemical Physics, 2014, 16, 5056.	2.8	5
53	High electrochemical performance and phase evolution of magnetron sputtered MoO <sub>2</sub> thin films with hierarchical structure for Li-ion battery electrodes. Journal of Materials Chemistry A, 2014, 2, 4714-4721.	10.3	49
54	Augmenting interventional ultrasound using statistical shape model for guiding percutaneous nephrolithotomy: Initial evaluation in pigs. Neurocomputing, 2014, 144, 58-69.	5.9	2

ZHI-CHENG LI

#	ARTICLE	IF	CITATIONS
55	Stability analysis and <mmi:math xmins:mmi="http://www.w3.org/1998/Math/Math/Math/Math/Math/Math/Math/Math&lt;/td"><td>nl:മാ⊗ <td>nml<mark>an</mark>row&gt; </td></td></mmi:math>	nl:മാ⊗ <td>nml<mark>an</mark>row&gt; </td>	nml <mark>an</mark> row>
56	Microstructure evolution of Li uptake/removal in MoO2@C nanoparticles with high lithium storage performance. Materials Research Bulletin, 2014, 50, 95-102.	5.2	18
57	An optical tracker based robot registration and servoing method for ultrasound guided percutaneous renal access. BioMedical Engineering OnLine, 2013, 12, 47.	2.7	15
58	Supine Lithotomy versus Prone Position in Minimally Invasive Percutaneous Nephrolithotomy for Upper Urinary Tract Calculi. Urologia Internationalis, 2013, 91, 320-325.	1.3	22
59	Segmentation of kidneys from computed tomography using 3D fast GrowCut algorithm. , 2013, , .		5
60	One-pot hydrothermal synthesized MoO2 with high reversible capacity for anode application in lithium ion battery. Electrochimica Acta, 2013, 102, 429-435.	5.2	77
61	Nonâ€ideal iris segmentation using anisotropic diffusion. IET Image Processing, 2013, 7, 111-120.	2.5	18
62	Segmentation of Kidneys from Computed Tomography Using 3D Fast GrowCut Algorithm. Applied Mechanics and Materials, 2013, 333-335, 1145-1150.	0.2	3
63	Dynamic Propagation Channel Characterization and Modeling for Human Body Communication. Sensors, 2012, 12, 17569-17587.	3.8	35
64	A pilot study on simulation of Ultrasound from MRI using ray-based model. , 2012, , .		0
65	Three dimensional ultrasound guided percutaneous renal puncture: A phantom study. , 2012, , .		2
66	Registration of Magnetic Resonance and 3D Ultrasound for Renal Intervention. , 2012, , .		0
67	Evaluation of 3D correspondence methods for building point distribution models of the kidney. , 2012, , .		2
68	Realization of spatial compliant virtual fixture using eigenscrews. , 2012, 2012, 1506-9.		2
69	Understanding the influence of alendronate on the morphology and phase transformation of apatitic precursor nanocrystals. Journal of Inorganic Biochemistry, 2012, 113, 1-8.	3.5	14
70	Augmenting intraoperative ultrasound with preoperative magnetic resonance planning models for percutaneous renal access. BioMedical Engineering OnLine, 2012, 11, 60.	2.7	17
71	Electrical properties of hexagonal BaTi1â^'x Fe x O3â^'δ (xÂ=Â0.1, 0.2, 0.3) ceramics with NTC effect. Journal of Materials Science: Materials in Electronics, 2012, 23, 1306-1312.	2.2	20

1D Infrared Camera Distortion Based on Polynomial Model. , 2012, , .

Zhi-Cheng Li

#	Article	IF	CITATIONS
73	Video Quality in Transmission over Burst-Loss Channels: A Forward Error Correction Perspective. IEEE Communications Letters, 2011, 15, 238-240.	4.1	15
74	Saliency and Gist Features for Target Detection in Satellite Images. IEEE Transactions on Image Processing, 2011, 20, 2017-2029.	9.8	167
75	Visual attention guided bit allocation in video compression. Image and Vision Computing, 2011, 29, 1-14.	4.5	191
76	Ultrasound-based surgical navigation for percutaneous renal intervention: In vivo measurements and in vitro assessment. , 2011, , .		7
77	Development and evaluation of ultrasound-based surgical navigation system for percutaneous renal interventions. , 2011, , .		3
78	Highly Efficient LaCoO <sub>3</sub> Nanofibers Catalysts for Photocatalytic Degradation of Rhodamine B. Journal of the American Ceramic Society, 2010, 93, 3587-3590.	3.8	59
79	A Multiple-Hop Synchronization Protocol with Packet Reconstitution. , 2010, , .		3
80	Optimized FEC based on distortion model for MVC streaming. , 2010, , .		2
81	Research on INS/terrestrial Pseudo-Range Integrated Navigation. , 2010, , .		0
82	Perceptual quality optimized FEC for video streaming. , 2010, , .		0
83	Modeling of distortion caused by Markov-model burst packet losses in video transmission. , 2009, , .		6
84	Efficient rate control scheme for low bit rate H.264/AVC video coding. Journal of China Universities of Posts and Telecommunications, 2009, 16, 103-107.	0.8	2
85	Modeling and Analysis of Distortion Caused by Markov-Model Burst Packet Losses in Video Transmission. IEEE Transactions on Circuits and Systems for Video Technology, 2009, 19, 917-931.	8.3	30
86	Dynamic end-to-end optimization for quality of transmission in reconfigurable transparent optical networks. Journal of Optical Networking, 2008, 7, 573.	2.5	9
87	Modeling of distortion for arbitrary packet loss patterns in video transmission. , 2008, , .		0
88	Low delay and high quality scheme for H.264 video transmission. , 2008, , .		0
89	Carrier class metro ethernet services over T-MPLS packet transport network. , 2007, , .		0
90	A hardware design on node in transport MPLS packet network based on FPGA. , 2007, , .		2

A hardware design on node in transport MPLS packet network based on FPGA. , 2007, , . 90

6

#	Article	IF	CITATIONS
91	Radiomic Features from Multi-Modal MRI Combined with Clinical Parameters Predict Molecular Subgroups in Patients with Medulloblastoma. SSRN Electronic Journal, 0, , .	0.4	0